

# First- and second-order statistical characterizations of the dynamic body area propagation channel of various bandwidths

David B. Smith · Leif W. Hanlen · Jian (Andrew) Zhang · Dino Miniutti · David Rodda · Ben Gilbert

Received: 30 November 2009 / Accepted: 7 December 2010  
© Institut Télécom and Springer-Verlag 2010

**Abstract** Comprehensive statistical characterizations of the dynamic narrowband on-body area and on-body to off-body area channels are presented. These characterizations are based on real-time measurements of the time domain channel response at carrier frequencies near the 900- and 2,400-MHz industrial, scientific, and medical bands and at a carrier frequency near the 402-MHz medical implant communications band. We consider varying amounts of body movement, numerous transmit–receive pair locations on the human body, and various bandwidths. We also consider long periods, i.e., hours of everyday activity (predominantly

indoor scenarios), for on-body channel characterization. Various adult human test subjects are used. It is shown, by applying the Akaike information criterion, that the Weibull and Gamma distributions generally fit agglomerates of received signal amplitude data and that in various individual cases the Lognormal distribution provides a good fit. We also characterize fade duration and fade depth with direct matching to second-order temporal statistics. These first- and second-order characterizations have important utility in the design and evaluation of body area communications systems.

**Keywords** Body area networks · Channel modeling · Akaike information criterion · Fading channels · Radio propagation · Wireless communication

---

Parts of this work appeared in [1–7].

---

D. Smith, L. Hanlen, J. (A.) Zhang, and D. Miniutti also hold adjunct appointments with the Australian National University.

---

National ICT Australia is funded by the Australian Government as represented by the Department of Broadband, Communications and the Digital Economy and the Australian Research Council through the ICT Centre of Excellence program.

---

D. B. Smith (✉) · L. W. Hanlen · D. Miniutti · D. Rodda  
National ICT Australia (NICTA), Locked Bag 8001,  
Canberra, ACT 2601, Australia  
e-mail: David.Smith@nicta.com.au

---

J. (A.) Zhang  
ICT Centre, CSIRO, P.O. Box 76, Epping, NSW 1710,  
Australia

---

B. Gilbert  
Air-Services Australia, GPO Box 367, Canberra,  
ACT 2601, Australia

## 1 Introduction

Current sensors and actuators are sufficiently small that they may be (relatively) unobtrusively attached to the human body. Wireless communication between such devices inspires the need for a wireless body area network (BAN) [8].

Applications for BANs [9] include bio-medical, sporting, and military uses, with medical likely to be the first substantial use. The close proximity of transceivers to the human body, as well as the need for long BAN lifetime, forces a low-power approach to any BAN and demands the wireless channel be well understood: so BAN transceivers may take full advantage of their environment [10].

Understanding the wireless channel implies detailed models which incorporate path-loss and power-delay profile of both narrowband and wideband wireless

BAN's at industrial, scientific, and medical (ISM) frequencies [11, 12] as well as the movement of the body [13].

A narrowband BAN point-to-point link may be viewed as an additive white Gaussian noise channel, with (time-varying) channel gain  $\alpha$ .

The objective of this work is to observe the dominant influences of the channel, specifically:

Can the (narrowband) BAN radio channel be characterized using well known statistical fading models?

1. What is the dominant first-order statistical model of the BAN channel?
2. Does this statistical model change according to scenario, transceiver location, bandwidth, and carrier frequency?
3. Can second-order variations of this model be characterized by using (the same) well-known statistical fading models, applied directly to the measured second-order statistics?

The static human body radio channel is well approximated by a uniform cylinder of "salty" water, hence the well-known SALTY model [14]. Path-loss only models match well to expectations from detailed electromagnetic models [15].

There has been various work on the macroscopic statistical properties of the human-radio channel, dominated by propagation characteristics, e.g., [16–20]. Various distributions have been suggested for mobile BAN channels, such as the Rician distribution [21], and the mixed parameter  $\kappa - \mu$  distribution [22]. In [23], a number of measurements were taken for the ultra-wideband BAN, and Lognormal fading was found between most transmit–receive pair (Tx–Rx) pairs for a stationary subject. A Nakagami- $m$  model was a poor fit to stationary models, suggested in [23], but a good fit for models involving arm movement; conversely, [24] observed strong matching to the Nakagami- $m$  model. Conversely, we find some instances where a Nakagami- $m$  model provides a good fit, but many instances where this is not the case. In [23], some measurements could not distinguish between Rayleigh and other models, with Rayleigh often close to best fit. We find Rayleigh distribution to consistently provide a poor fit. We also postulate that median path loss is a better guide for a BAN communications operating point than mean path loss, in consideration of all signal measurements; to the best of our knowledge, this has not been reported by others with respect to body area communications.

We evaluated several on-body and off-body propagation scenarios, incorporating varying amounts of

movement. These scenarios incorporate a range of carrier frequencies, near 400, 900, and 2,400 MHz, and different communications bandwidths. The complete set contains more than 20 subjects and many tens of hours of measurements.

Several statistical models tested against the measured data. We outline each and provide a brief explanation as to why each was chosen as a potential candidate:

- *Normal (and Rayleigh)* are well-known for their maximum entropy characteristics. Channels which have no significant structure are well modeled by these distributions.
- *Lognormal* distribution arises from a law-of-large numbers approach to multiplicative effects and is commonly used to model shadowing (long-term fading processes) in terms of the average power received.
- *Nakagami- $m$*  is a common model used in mobile fading. It includes Rayleigh as a special case and may be used to approximate Rician distributions. The *Gamma* distribution [25] is a more efficient model over Nakagami- $m$  in mobile fading channels. When Nakagami- $m$  is a poor fit for channel statistics, Rician will also be a poor fit.
- *Weibull* has been used for multipath modeling and is generally found to model small-scale fading and multipath inter-arrival [26] processes well. It also includes Rayleigh as a special case.

We have investigated best fits of the models above as:

- *First-order fits*—measured data are fit directly against the test densities.
- *Second-order fits*—second-order statistics of the measured data, e.g., fade durations and magnitudes of fades, are fit to the test densities.

This approach allows us to investigate the temporal dependence of the signal, without requiring a complete conditional probability density to be formulated. An approximate average Doppler spread for each agglomerate very narrowband on-body area propagation scenario is also derived from the average level crossing rates.

A description of the experimental setup for four different scenarios follows in the next section. Section 3 gives a detailed description of the modeling of the received signal amplitude in the dynamic narrowband and very-narrowband on-body and off-body area channel, with comprehensive characterization and some general

observations. Section 4 gives a brief description of some second-order statistics and their characterization and draws inferences. Finally, Section 5 provides concluding remarks, including various general observations inferred from our measurement campaign.

## 2 Experimental setup

The experimental setup encapsulated four separate measurement scenarios, where each scenario contained a number of measurement sets. In brief, these measurement scenarios were discussed below.

### 2.1 Summary of experimental setup

1. On-body<sup>1</sup> characterization with several transceiver (Tx/Rx) locations and defined movement, i.e., standing still, slow walking, and fast-jogging “on-the-spot” in an indoor office. These characteristics are measured near 400, 900, and 2,400 MHz. Measurements are made with several bandwidths (10 MHz and 100 kHz).
2. Off-body<sup>2</sup> communications with a Tx on the subject’s body, several distances of Tx to Rx off the body, several orientations of Tx with respect to Rx, different positions of Tx on the subject’s body, and with the subject walking and standing (performed for 10 MHz and 100 kHz bandwidths).
3. On-body with various human subjects moving at four different set speeds on a treadmill, in an indoor office at a carrier frequency near 900 MHz (100 kHz bandwidth). The channel is characterized using a number of adult human subjects.
4. On-body for every-day activity of long periods using small body-mounted radios/channel sounders as Tx and Rx, with multiple (small) radios simultaneously mounted on the human body. This every-day activity predominantly encompasses activity of an office worker over several hours in an indoor office, at home, and jogging in an outdoor suburban environment. The measurements were made near 2,400 MHz with 540 kHz bandwidth.

### 2.2 Details of the experimental setup

For the first three measurement cases (those apart from measurement using the channel sounders), wireless on-

<sup>1</sup>On-body implies transmission and reception both on the subject’s body.

<sup>2</sup>Off-body implies transmission on the subject’s body and reception somewhere off the subject’s body.

body channel measurements were made in the same indoor office environment, using two antennas (one Tx, one Rx) strapped with VELCRO® tape to the body of eight adult test subjects, two females and six males. The antennas were Octane BW-800-900, dimensions 71 mm (length) × 71 mm (width) × 12.7 mm (depth), and Octane BW-2400-2500, dimensions 91 mm (l) × 84 mm (w) × 7.6 mm (d), wearable flexible antennas for 900 and 2,400 MHz, and Comet SMA-501 helical stub antennas, dimensions 46 mm (l) × 12 mm (w) for 400 MHz. The Octane antennas are approximately omnidirectional, with similar radiation patterns in both E- and H-planes. The Comet SMA-501 antenna has 0-dBi gain and is assumed omnidirectional in the H-plane. Thus, in all experiments, the antenna pattern was omnidirectional in the plane tangential to the body surface. The antennas were worn such that the E-plane of the antennas was in the vertical up-down direction, i.e., perpendicular to the floor of the environment. In all cases, the antennas were placed directly on the subject’s body, with only separation due to the width of clothing. The antennas are considered part of the channel. In the first three measurement cases, a vector signal analyzer (VSA) was used, and due to the nature of the VSA measurements, the signal was always above the noise floor.

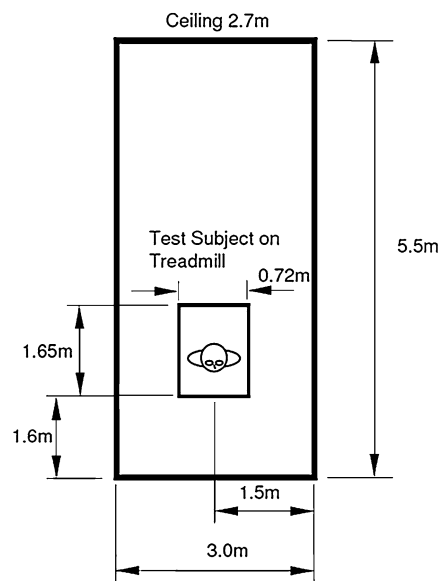
1. **On-body 10 MHz bandwidth** Channel measurements were performed by transmitting test signals emanating from a VSA centered in regions around the 400-, 900-, and 2,400-MHz ISM bands, specifically 427, 820, and 2,360 MHz. The test signals were separately transmitted from one antenna while the 181.5-cm/78-kg male test subject performed three different actions: (1) standing still, (2) walking on the spot, and (3) running on the spot. The signal received at the other antenna was down-converted, sampled for approximately 10 s, and saved to disk. Analysis of the measurements was later done offline.

Appropriate choices were made when choosing the bit rate (12.5 Mbps), modulation scheme (BPSK), and pulse shaping filters (root raised-cosine). The combination used provided a relatively flat (1 dB attenuation in the sidelobes) signal spectrum over a 10-MHz bandwidth. A wireless system with 1-bit/s/Hz spectral efficiency could provide the 10 Mbps required by the 802.15.6 technical requirements document [8] within this bandwidth. The complex channel gain was sampled over 2,048 bits every 2.5 ms.

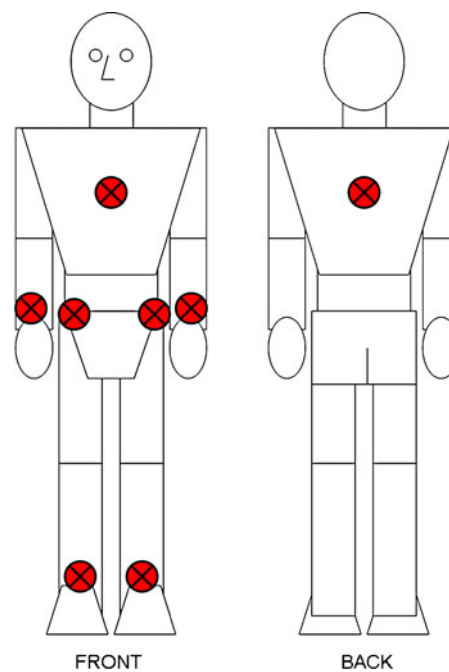
**100 kHz bandwidth equivalent** In these studies, we transmitted a pure carrier (or tone), i.e., with no modulation, at 2,360 and 427 MHz. The received signal

was sampled continuously at 100 ksamples per second. Thus, if this sampling rate was adopted in a wireless

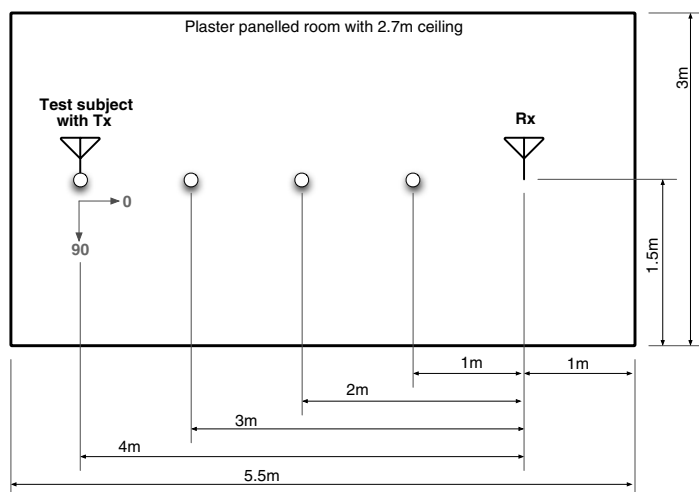
system with 1 bit/sample and with a 1-bit/s/Hz spectral efficiency, this is equivalent to a 100-kHz bandwidth.



(a) On-Body Experimental treadmill environment, including subject location



(b) Antenna positions on test subjects



(c) Off-Body Experimental environment. An angle of  $0^\circ$  corresponds to the test subject facing the receive antenna



(d) Treadmill photo

**Fig. 1** Experimental on-body and off-body environments, with transceiver positions on test subject. **a** On-body experimental treadmill environment, including subject location. **b** Antenna

positions on test subjects. **c** Off-body experimental environment. An angle of  $0^\circ$  corresponds to the test subject facing the receive antenna. **d** Treadmill photo

The received signal amplitude was recorded every millisecond; hence, this measurement was based on downsampling and an averaging over 100 samples.<sup>3</sup> Measurements were made over a period of 20 s.

**2. Off-body** Wireless on-body to off-body channel measurements were made using a commercial wearable antenna at the three previous frequencies, 427, 820, and 2,360 MHz, with the same test subject over periods of 5 s for 10 MHz bandwidth and 20 s for 100 kHz bandwidths. For both cases of 10 MHz bandwidth measurements and 100 kHz bandwidth measurements:

- The transmit antenna, Tx, was placed at two locations on the test subject: front of chest and right wrist, and the receive antenna, Rx, was placed on an aluminum tripod that was fitted with a perspex stand to hold the receive antenna. Thus, the stand holding Rx was not a source of reflection/diffraction, and any reflections from the tripod were considered part of the channel and importantly are in the far field and hence did not significantly change radiation pattern characteristics of the Rx antenna.
- Measurements were taken with a VSA with the test subject standing in four different locations in the room. The horizontal distance between the test subject and Rx was either 1, 2, 3, or 4 m at these locations. At each location, measurements were taken with the subject facing in four different directions: 0°, 90°, 180°, and 270°, with 0° representing the subject facing the receive antenna and 90° representing the subject moved 90° clockwise with respect to the Rx.
- For each orientation and location in the room, measurements were taken with the subject standing still and walking on the spot and the total duration of each measurement was 5 s.

All other parameters for larger bandwidth are the same as case 1 for larger bandwidth; similarly all other parameters for smaller bandwidth are the same as case 1 for smaller bandwidth.

**3. On-body treadmill 100 kHz bandwidth equivalent** measurements were performed using the VSA based on subject movement on a treadmill in an indoor office environment at four different set speeds 3, 6, 9, and 12 km/h, hence emulating walking, jogging, and running with each measurement set being taken over a period of 60 s (i.e., 60,000 samples). Overall approximately

3.5 h of data was captured. As part of the channel, the treadmill had holding arms, which were partially metallic and partially plastic.

For cases 1 and 3, transmitting and receiving antennas were strapped to different locations on the test subject's body. The location and lay-out within the indoor office environment is illustrated in Fig. 1a for on-body treadmill measurements and Fig. 1c for off-body measurements, and Fig. 1b illustrates the locations of the antennas on the test subject/s for on-body measurements and a photo of the treadmill, with a running subject, is shown in Fig. 1d. Table 1 lists the combinations of transmit and receive antenna locations used for on-body measurements, with separate channel measurements made for each combination. For reasons of symmetry, the left wrist and left ankle to chest measurements were not recorded.

**4. On-body channel sounder 540 kHz bandwidth** The final measurement case used channel sounders that were small radios placed on ten adult test subjects where the radios used a Chipcon CC2500 2.4-GHz low-power transceiver; an Atmega 1281 microcontroller used to control the transceiver, including MAC layer control and frame-control; a ceramic multilayer chip antenna from Phycomp which is omnidirectional in the H-plane, had a gain of 1.2 dBi, dimensions 7.4 mm (l) × 5.5 mm (w) × 1.3 mm (d), and was operational at 2.4 GHz; an SD card used to log the data; and a battery with a lifetime of 8–12 h. Subjects wore a varying amount of these channel sounders operating at 2.36 GHz, with some operating as Rx, some as Tx and Rx, and some as Tx (the total amount of Tx and Rx varied from 3 to 20). An image of the channel sounder is shown in Fig. 2.

Individual subject measurements generally lasted for a period of 2 hours or more, while subjects were engaged in everyday activity (often indoors, such as in an office, but also engaged in other activities such as jogging outdoors). Received signal amplitude measurements and hence channel gain measurements were made in this case using the received signal strength indicator (RSSI) log made upon successful packet detection

**Table 1** Matrix of transmit and receive antenna locations for on-body measurements in scenarios 1 and 3

| Receiver location | Transmitter location |    |    |    |    |   |
|-------------------|----------------------|----|----|----|----|---|
|                   | C                    | Rw | Lw | Ra | La | B |
| Rh                | ×                    | ×  | ×  | ×  | ×  | × |
| C                 |                      | ×  |    | ×  |    | × |

× the corresponding channel measurement was conducted, C chest, Rw right wrist, Lw left wrist, Ra right ankle, La left ankle, B back, Rh right hip

<sup>3</sup>One advantage of this averaging is that it enables the capture of far deeper fades.

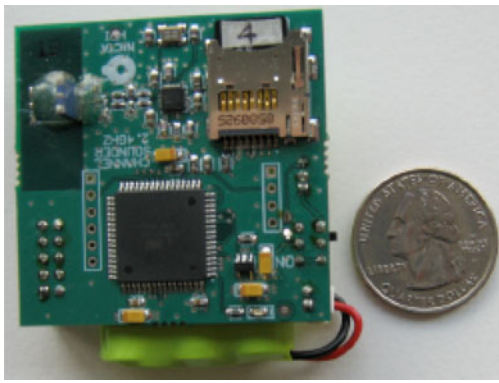


**Fig. 2** Picture of the channel sounder used in measurement case 4

by the CC2500 radios. The channel sounder recorded measurements in steps of 0.5 dB. The CC2500 radios have a Rx sensitivity less than  $-100$  dBm (with the radios tuned to a Tx power of 0 dBm or 1 mW), i.e., an approximate noise floor of  $-100$  dB. The data rate was 250 kbps, and the Rx bandwidth for the channel sounder was 540 kHz. With one operational Tx, the RSSI was logged at the Rx every 5 ms; with two simultaneous Tx, the RSSI was logged at the Rx every 10 ms. A total of 140 Tx/Rx link measurements were made for the ten different adult test subjects for the channel sounder measurements.

### 3 First-order statistical modeling of received signal amplitude distribution

In this section, we attempt to define some reliable statistical models for agglomerate receive signal amplitude distributions over the different scenarios and the four measurement cases, with and without subject movement, and for long periods of every-day using channel sounder.

Firstly, for all measurements, scenarios, and cases, the measured received signal amplitude across one set of measurements (e.g., say from Tx at right wrist to Rx at chest for narrowband) for a given link-measurement was normalized according to the square root of the mean power for that link measurement. This enabled agglomeration for given scenarios and the fitting of distributions to sets of agglomerate data. We choose this agglomeration because we are seeking an indicator of a general scenario, which is a rough approximate to any link, given a particular dynamic (e.g., standing or walking or running) and a given carrier frequency.

We obtained maximum likelihood estimates of received signal amplitude data (thus, data  $x > 0$ ) for these

six common distributions often used in channel characterization and modeling, where agglomerate receive signal amplitude data has a common mean of 1:

- Normal with probability density function (PDF)

$$f(x|\mu, \sigma) = \frac{1}{\sigma\sqrt{2\pi}} \exp\left\{-\frac{(x - \mu)^2}{2\sigma^2}\right\} \quad (1)$$

- Lognormal

$$f(x|\mu, \sigma) = \frac{1}{x\sigma\sqrt{2\pi}} \exp\left\{-\frac{(\ln(x) - \mu)^2}{2\sigma^2}\right\} \quad (2)$$

where  $\ln(\cdot)$  is the natural logarithm.

- Gamma

$$f(x|a, b) = \frac{1}{b^a\Gamma(a)} x^{a-1} \exp\left\{-\frac{x}{b}\right\} \quad (3)$$

where  $\Gamma(\cdot)$  is the Gamma function

- Nakagami-m

$$f(x|m, \omega) = \frac{2m^m}{\Gamma(m)} \frac{x^{2m-1}}{\omega^m} \exp\left\{-\frac{m}{\omega}x^2\right\} \quad (4)$$

- Weibull

$$f(x|a, b) = b a^{-b} x^{b-1} \exp\left\{-(x/a)^b\right\} \quad (5)$$

- Rayleigh

$$f(x|b) = \frac{x}{b^2} \exp\left\{-\frac{x^2}{2b^2}\right\} \quad (6)$$

In order to compare between the six distributions, we choose the Akaike information criterion (AIC) [27], as used in [23] for wideband characterization, to choose the best fitting distributions for our dynamic narrowband characterization.

The second-order AIC ( $AIC_c$ ) is given by

$$AIC_c = -2 \ln(l(\hat{\theta}|\text{data})) + 2K + \frac{2K(K+1)}{(n-K-1)} \quad (7)$$

where  $\ln(l(\hat{\theta}|\text{data}))$  is the value of the maximized log-likelihood over the unknown parameters ( $\theta$ ), given the data and the model,  $K$  is the number of parameters estimated in the model, and  $n$  is the sample size. We find the maximized log likelihood from the ML estimates. The Akaike information criterion can be used as a relative measure, such that the model with the lowest  $AIC_c$  approximates the “best” distribution out of the models tested. Thus, this criterion provides the model with the minimum loss of information out of those tested.

**Table 2** Agglomerate scenarios and the best fitting model with parameters (in brackets) and the  $\Delta AIC_c$  to the next best-fitting model, to those scenarios at 427 MHz, 820 MHz, and 2.36 GHz

| Channel  | Action     | Freq. (MHz) | BW      | Distribution                                     | $\Delta AIC_c$ |
|----------|------------|-------------|---------|--|----------------|
| On-body  | Moving     | 427         | 10 MHz  | Gamma ( $a = 3.41, b = 0.259$ )                  | 1,555          |
| On-body  | Moving     | 820         | 10 MHz  | Gamma ( $a = 2.97, b = 0.291$ )                  | 1,983          |
| On-body  | Moving     | 2,360       | 10 MHz  | Weibull ( $a = 0.978, b = 1.82$ )                | 1.6            |
| On-body  | Moving     | 427         | 100 kHz | Gamma ( $a = 2.78, b = 0.31$ )                   | 11,286         |
| On-body  | Moving     | 2,360       | 100 kHz | Nakagami-m ( $m = 0.65, \omega = 1$ )            | 822            |
| On-body  | Moving     | 820         | 100 kHz | Weibull ( $a = 0.996, b = 1.97$ )                | 4,791          |
| On-body  | Standing   | 427         | 10 MHz  | Weibull ( $a = 1.04, b = 12.3$ )                 | 3,149          |
| On-body  | Standing   | 820         | 10 MHz  | Gamma ( $a = 203, b = 0.00492$ )                 | 105            |
| On-body  | Standing   | 2,360       | 10 MHz  | Gamma ( $a = 77.4, b = 0.0128$ )                 | 29.2           |
| On-body  | Standing   | 427         | 100 kHz | Normal ( $\mu = 0.99, \sigma = 0.14$ )           | 19,501         |
| On-body  | Standing   | 2,360       | 100 kHz | Normal ( $\mu = 0.974, \sigma = 0.227$ )         | 651            |
| On-body  | Walking    | 427         | 10 MHz  | Nakagami-m ( $m = 1.3, \omega = 1$ )             | 250            |
| On-body  | Walking    | 820         | 10 MHz  | Gamma ( $a = 3.52, b = 0.251$ )                  | 1,092          |
| On-body  | Walking    | 2,360       | 10 MHz  | Weibull ( $a = 1.01, b = 2.05$ )                 | 8.3            |
| On-body  | Walking    | 427         | 100 kHz | Gamma ( $a = 3.08, b = 0.285$ )                  | 2,066          |
| On-body  | Walking    | 2,360       | 100 kHz | Weibull ( $a = 0.955, b = 1.68$ )                | 258            |
| On-body  | Running    | 427         | 10 MHz  | Gamma ( $a = 2.84, b = 0.302$ )                  | 1,357          |
| On-body  | Running    | 820         | 10 MHz  | Gamma ( $a = 2.59, b = 0.327$ )                  | 904            |
| On-body  | Running    | 2,360       | 10 MHz  | Weibull ( $a = 0.948, b = 1.64$ )                | 79.8           |
| On-body  | Running    | 427         | 100 kHz | Gamma ( $a = 2.55, b = 0.333$ )                  | 8,426          |
| On-body  | Running    | 2,360       | 100 kHz | Nakagami-m ( $m = 0.567, \omega = 1$ )           | 1,131          |
| On-body  | Various-CS | 2,360       | 540 kHz | Gamma ( $a = 1.31, b = 0.562$ )                  | 5,970          |
| Off-body | Moving     | 820         | 10 MHz  | Weibull ( $a = 1.05, b = 3.04$ )                 | 284            |
| Off-body | Moving     | 2,360       | 10 MHz  | Nakagami-m ( $m = 1.6, \omega = 1$ )             | 227            |
| Off-body | Moving     | 427         | 100 kHz | Weibull ( $a = 1.02, b = 2.25$ )                 | 59,507         |
| Off-body | Moving     | 2,360       | 100 kHz | Weibull ( $a = 1.01, b = 2.15$ )                 | 18,537         |
| Off-body | Standing   | 820         | 10 MHz  | Lognormal ( $\mu = -0.000839, \sigma = 0.0289$ ) | 202            |
| Off-body | Standing   | 2,360       | 10 MHz  | Gamma ( $a = 384, b = 0.0026$ )                  | 70.4           |
| Off-body | Standing   | 427         | 100 kHz | Gamma ( $a = 44, b = 0.0224$ )                   | 40,281         |
| Off-body | Standing   | 2,360       | 100 kHz | Normal ( $\mu = 0.987, \sigma = 0.161$ )         | 7,906          |

Various-CS channel sounder measurements, BW bandwidth, Freq. frequency

We note that from our measurements, for each agglomeration, the sample size  $n$  is constant for comparing between distributions, and  $K = 2$  for all distributions apart from the Rayleigh distribution for which  $K = 1$ . Thus, in effect we can use the  $AIC_c$  to distinguish between a Rayleigh model and the five other models. To compare between the five other models, we consider the maximized log-likelihood score.

We stress that *in no case does the Rayleigh model provide the best fit*, either for individual scenarios or agglomerate scenarios, for the measured normalized received signal amplitude data across all scenarios at 427, 820, and 2,360 MHz in terms of the  $AIC_c$ .

### 3.1 Agglomerate-data first-order statistical analysis—results

The distributions, or models, that are the best fitting distributions across agglomerate scenarios, according to ML estimates and the subsequent  $AIC_c$ , are given in

Table 2.<sup>4</sup> Note that the most common best-fitting distributions of the 29 agglomerate scenarios are Gamma distribution (best fit in 12 cases) and the Weibull distribution (best fit in nine cases). For reference  $\Delta AIC_c$ , the difference between  $AIC_c$  of the best-fitting model and that of  $AIC_c$  of the next best-fitting model is also given in this table, demonstrating in most cases the clear superiority of the best model. As it is noted that a  $\Delta AIC_c > 10$ , [28] indicates a poor support for the alternate model.

We propose that for these data the  $AIC_c$  is a more reliable indicator for a range of models than a hypothesis test, which can only pass or fail a particular model with an arbitrary significance level. Further standard

<sup>4</sup>Variance of Gamma, Weibull, and Nakagami-m distributions, based on their respective distribution parameters, are given in “Appendix”.

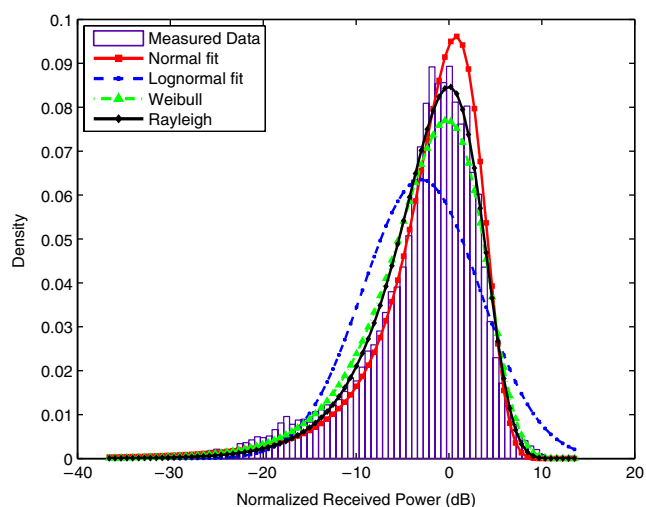


**Fig. 3** PDF on-body agglomerate measurements of normalized (to mean) received power for subject moving, 10 MHz bandwidth, at 2,360 MHz

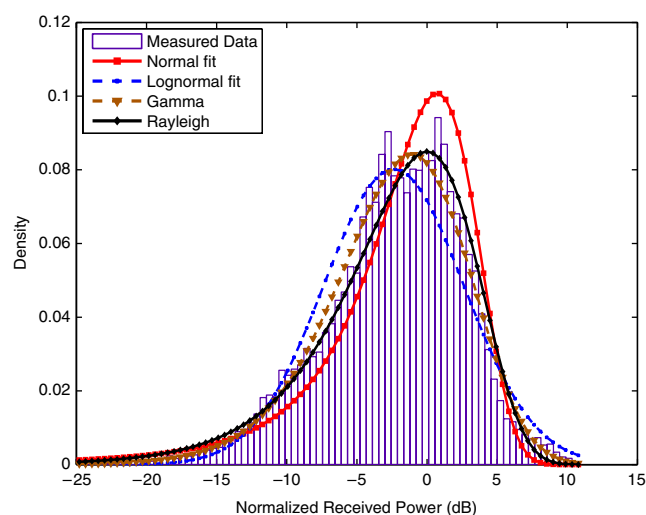


**Fig. 5** PDF on-body agglomerate of subject walking, 10 MHz bandwidth, at 820 MHz

goodness-of-fit measures, such as chi-square goodness-of-fit, assume a normal distribution of model errors with respect to the data, which was not observed here.

We note for the classification of action in Table 2 that for “on-body” channels, “moving” implies both walking and running, whereas for “off-body” channels moving implies “walking”. Further, we note that the treadmill measurements are described by the “moving” case with 100 kHz (equivalent) bandwidth at 820 MHz.

In the following figures, we show plots of the empirical PDF for various agglomerate scenarios represented in Table 2. The bin size for the histogram used

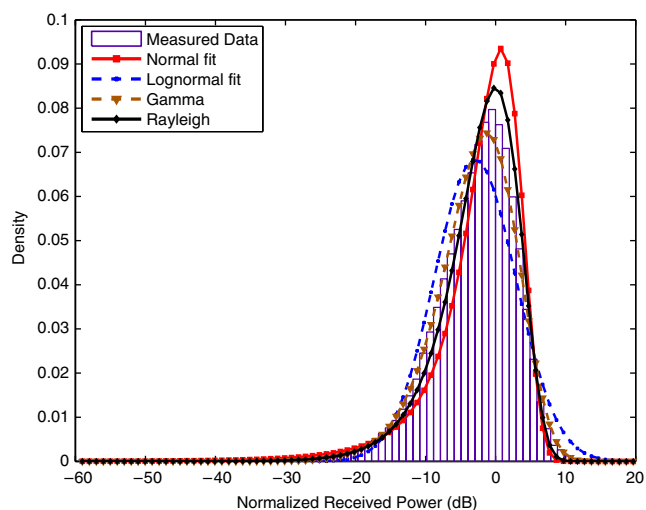


**Fig. 4** PDF on-body agglomerate of subject moving, 100 kHz bandwidth, at 427 MHz

to describe the PDF from the measured data is chosen according to the “Freedman–Diaconis” rule<sup>5</sup> [29]. Figures 3, 4, 5, 6, 7, 8, and 9 show empirical PDFs for various on-body, i.e., on→on-body, agglomerate scenarios with movement at the three carrier frequencies, at 10 MHz and 100 kHz bandwidths in Figs. 3, 4, 5, 6, and 7; the treadmill measurements are shown in Fig. 8; and channel sounder measurements are shown in Fig. 9. Overlaid on each empirical PDF is the PDF of the best fit for four distributions.<sup>6</sup> It is noteworthy that in all these cases the best fits are either Weibull or Gamma distributions; in all cases, the best-fitting distributions, with parameters given in Table 2, provide good fits, as evidence in the figures for on-body measurements. It is of special note that in Fig. 9, the Weibull and Gamma distributions both provide excellent fits to this very large agglomeration of data, representing a range of subjects, with many hours logged of data, which suggests that the generic body area channel can be well modeled using these distributions.

Figures 10, 11, and 12 show empirical PDFs for various off-body agglomerate scenarios with and without

<sup>5</sup>Bin size  $B_s$  given by

$$B_s = 2I_r(x)n^{-1/3}$$

where  $I_r$  is the inter-quartile range of the data sample  $x$  (in this case measured normalized received signal amplitude) and  $n$  is the sample size of  $x$ .

<sup>6</sup>Lognormal, Normal, and Rayleigh best-fit PDFs are overlaid, with the best of best fits between Weibull, Gamma, and Nakagami- $m$  PDFs also overlaid; in Fig. 9, Weibull and Gamma are overlaid.

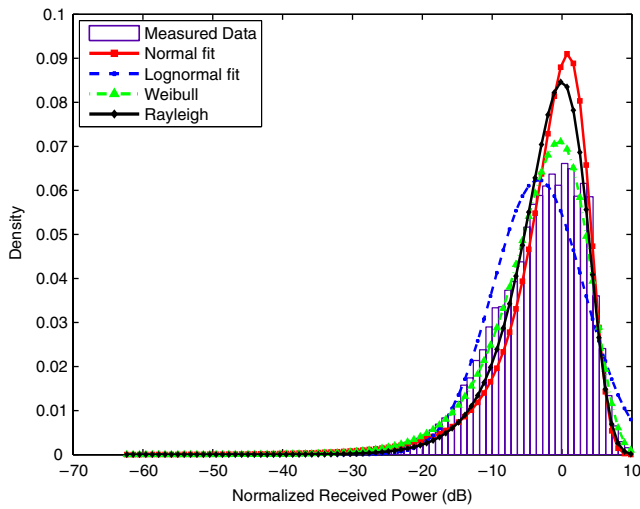


**Fig. 6** PDF on-body agglomerate of subject walking, 100 kHz bandwidth, at 2,360 MHz

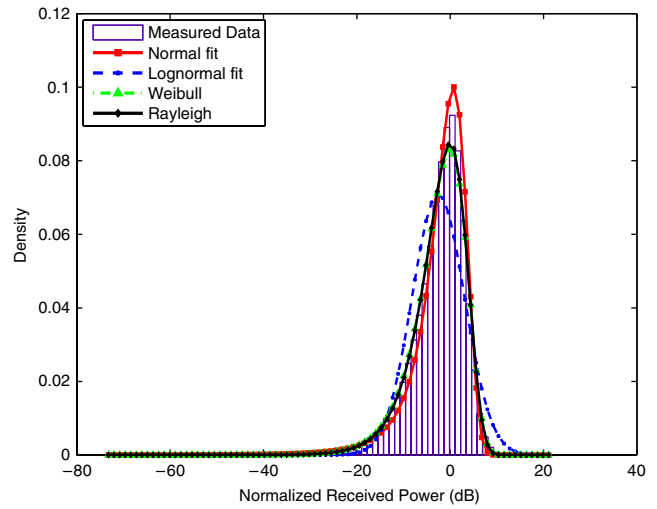


**Fig. 8** PDF on-body treadmill agglomerate of all subjects moving, 100 kHz bandwidth, at 820 MHz

movement, at 820 and 2,360 MHz at 10 MHz and 100 kHz bandwidth (results for 427 MHz show similar trends). It is noteworthy that in each of these cases, the best-fitting distribution varies; in the first off-body figure, Fig. 10, it is Weibull with the scenario of subject moving at the 10-MHz bandwidth and at the carrier frequency of 820 MHz; in the second off-body figure, Fig. 11, it is Gamma with the subject standing in the same measurement cases as Fig. 10; and in the third off-body figure, Fig. 12, it is Normal with the subject standing and a 100-kHz bandwidth at 2,360 MHz.

### 3.2 Agglomerate-data first-order statistical analysis—observations

A summary of the best-fitting models by distribution type, for which the parameters appear in Table 2, is given in Tables 3 and 4, for the case of distribution-type v. dynamic (e.g., walking or running) in Table 3, and the case of carrier frequency v. distribution type in Table 4, where the on-body and off-body cases are separated.

The Weibull and Gamma best fits, being the general best models, to fit agglomerate measurements underline their reliability in body area channels, similar to various other radio communications channels as generic models for small-scale fading [25, 26],

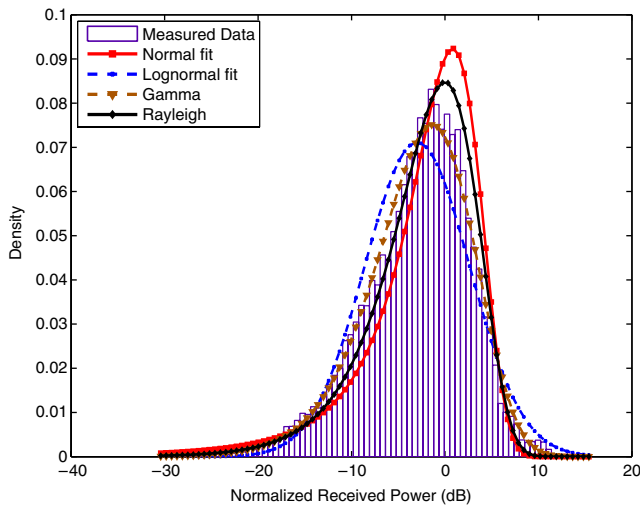


**Fig. 7** PDF on-body agglomerate of subject running, 10 MHz bandwidth, at 427 MHz

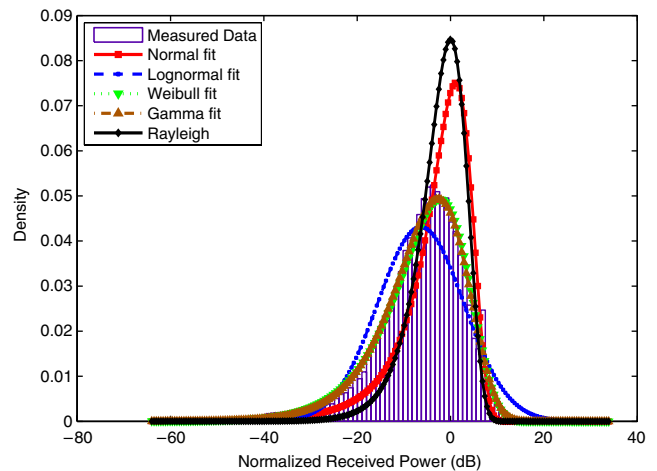


**Fig. 9** PDF on-body channel sounder agglomerate (capturing) everyday activity of ten subjects, 540 kHz bandwidth, at 2,360 MHz

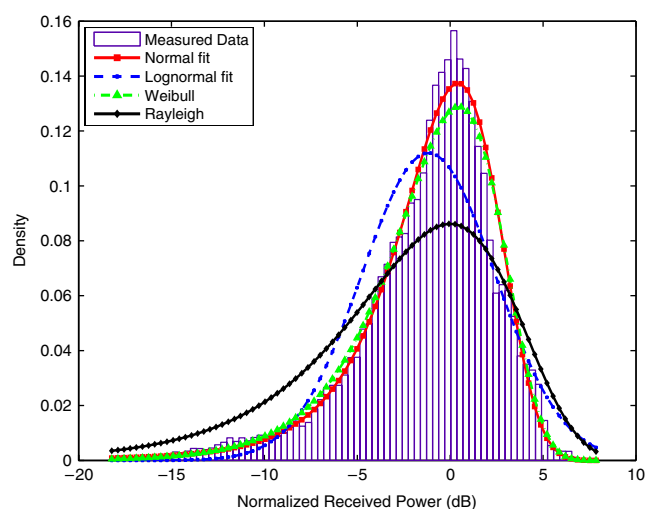


**Fig. 10** PDF off-body agglomerate of subject moving, 10 MHz bandwidth, at 820 MHz

particularly indoors [30], but also outdoors [31]. It is noted that in [32], a clear argument is made for a Gamma distribution to model “shadow fading”, or slow fading. It can be used for a fading channel with random number of paths (with negative binomial distribution) and nonuniform phase distributions [33]. It is clear that the generic on-body area channel, particularly where there is movement, and for typical everyday activity, can be well modeled using either a Weibull or Gamma distribution.

It seems that dominant statistical agglomerate models, i.e., Gamma and Weibull, are independent of scenario, i.e., such as on-body walking or off-body walking; bandwidth, whether larger narrowband bandwidth or

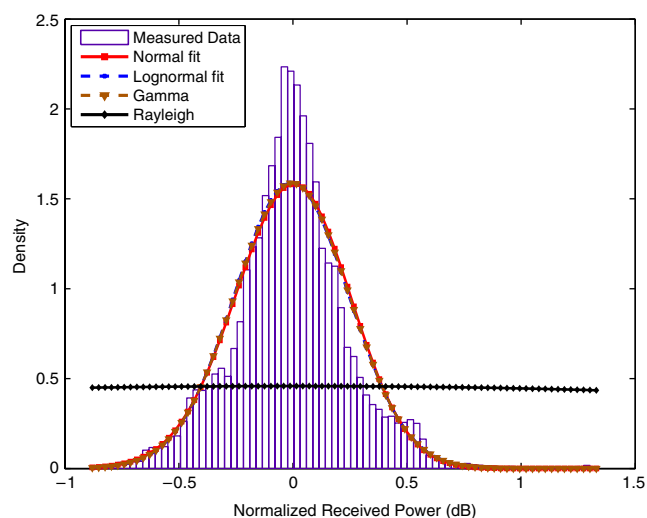


**Fig. 11** PDF off-body agglomerate of subject standing, 10 MHz bandwidth, at 820 MHz

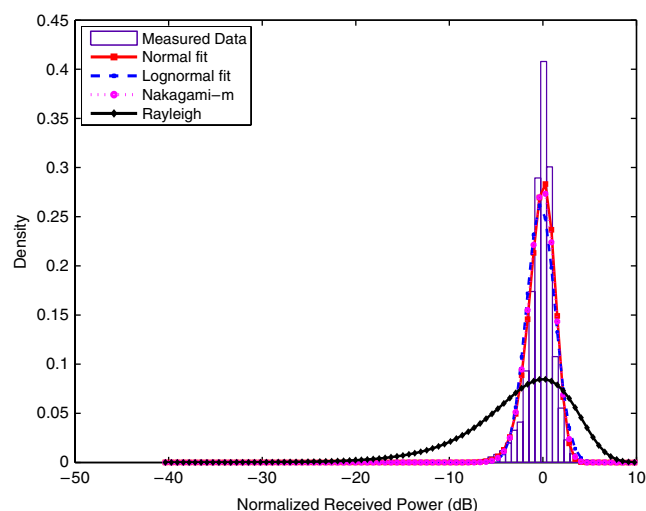


**Fig. 12** PDF off-body agglomerate of subject standing, 100 kHz bandwidth, at 2,360 MHz

smaller narrowband bandwidth; and carrier frequency. However, it can be observed, particularly from Table 2, that with increasing rate of subject movement, the shape parameter  $a$  of the Gamma distribution and the shape parameter  $b$  of the Weibull distribution both decrease, which indicate more severe fading as the amount of subject movement increases.

All first-order agglomerate statistical analysis was done with the mean removed, and this is appropriate for fading analysis made. However, *we postulate that if a typical path loss for a BAN channel, based on a number of on-body transceiver positions, is to be given, this should be the median path loss*, as the mean is skewed by larger receive signal amplitude values in a measurement set, where there is a large range over many orders of magnitude. For instance, in the case of the channel sounder data, the mean of the means of each link power measurement gives a path loss of 55.4 dB; however, the median of medians of each link measurement is 72 dB, which we believe is far more representative of general path losses for the on-body area channel at 2.4 GHz. The median path loss represents the value at which there are the same number of path losses greater than the median, as those path losses smaller than the median, whereas a much smaller fraction of path losses are greater than the mean value.

### 3.3 Individual link-data first-order statistical analysis—results

For individual scenarios, i.e., particular links best-fitting distributions were fitted to receive signal amplitude normalized to the maximum amplitude to that

**Table 3** Summary of best fitting agglomerate models to on-body and off-body data (distribution-type vs. dynamic)

|            | On-body |      |     |                   |         | Off-body |             |
|------------|---------|------|-----|-------------------|---------|----------|-------------|
|            | Stand   | Walk | Run | Move (walk + run) | Mixture | Stand    | Move (walk) |
| Gamma      | 2       | 2    | 3   | 3                 | 1       | 2        | 0           |
| Weibull    | 1       | 2    | 1   | 2                 | 0       | 0        | 3           |
| Lognormal  | 0       | 0    | 0   | 0                 | 0       | 1        | 0           |
| Normal     | 2       | 0    | 0   | 0                 | 0       | 1        | 0           |
| Nakagami-m | 0       | 1    | 1   | 1                 | 0       | 0        | 1           |
| Rayleigh   | 0       | 0    | 0   | 0                 | 0       | 0        | 0           |

**Table 4** Summary of best fitting agglomerate models to on-body and off-body data (carrier frequency vs. distribution-type)

|             | Gamma | Weibull | Lognormal | Normal | Nakagami-m | Rayleigh |
|-------------|-------|---------|-----------|--------|------------|----------|
| On-body     |       |         |           |        |            |          |
| 427—small   | 3     | 0       | 0         | 1      | 0          | 0        |
| 427—large   | 2     | 1       | 0         | 0      | 1          | 0        |
| 820—small   | 0     | 1       | 0         | 0      | 0          | 0        |
| 820—large   | 4     | 0       | 0         | 0      | 0          | 0        |
| 2,360—small | 1     | 1       | 0         | 1      | 2          | 0        |
| 2,360—large | 1     | 3       | 0         | 0      | 0          | 0        |
| Off-body    |       |         |           |        |            |          |
| 427—small   | 1     | 1       | 0         | 0      | 0          | 0        |
| 820—large   | 0     | 1       | 1         | 0      | 0          | 0        |
| 2,360—small | 0     | 1       | 0         | 1      | 0          | 0        |
| 2,360—large | 1     | 0       | 0         | 0      | 1          | 0        |

**Table 5** Sample of individual scenarios and the parameters (in brackets) of the best-fitting model, in each case lognormal, to those scenarios at 820 MHz and 2.36 GHz for on-body and 10 MHz bandwidth

| Tx location | Rx location | Action   | Lognormal distribution         |                                  |
|-------------|-------------|----------|--------------------------------|----------------------------------|
|             |             |          | 820 MHz                        | 2.36 GHz                         |
| Chest       | Right hip   | Standing | $\mu = -0.086, \sigma = 0.042$ | $\mu = -0.2015, \sigma = 0.0921$ |
| Left wrist  | Right hip   | Walking  | $\mu = -1.48, \sigma = 0.62$   | $\mu = -1.48, \sigma = 0.80$     |
| Back        | Right hip   | Running  | $\mu = -1.31, \sigma = 0.56$   | $\mu = -1.11, \sigma = 0.39$     |
| Back        | Chest       | Running  | $\mu = -2.55, \sigma = 0.51$   | $\mu = -0.60, \sigma = 0.24$     |
| Right wrist | Chest       | Running  | $\mu = -1.32, \sigma = 0.44$   | $\mu = -1.80, \sigma = 0.86$     |

**Table 6** Sample of individual scenarios and the best-fitting model, with parameters (in brackets) to the normalized signal amplitude data for those scenarios transmitting on-body, Tx, to Rx off-body at 820 MHz and 2.36 GHz at 10 MHz bandwidth

| Tx location | Action | D (m) | Angle (deg) | Distribution                                   |  |
|-------------|--------|-------|-------------|--|--|
|             |        |       |             | 820 MHz  | 2.36 GHz                                       |
| Chest       | Walk   | 2     | 180         | Lognormal ( $\mu = -0.905, \sigma = 0.361$ )   | Gamma ( $a = 20.9, b = 0.0295$ )               |
| Chest       | Walk   | 2     | 270         | Weibull ( $a = 0.769, b = 4.95$ )              | Gamma ( $a = 10.9, b = 0.0504$ )               |
| Chest       | Stand  | 4     | 0           | Lognormal ( $\mu = -0.0361, \sigma = 0.0154$ ) | Lognormal ( $\mu = -0.052, \sigma = 0.0157$ )  |
| Chest       | Stand  | 4     | 90          | Lognormal ( $\mu = -0.0285, \sigma = 0.0156$ ) | Lognormal ( $\mu = -0.151, \sigma = 0.0793$ )  |
| Right wrist | Walk   | 1     | 0           | Nakagami-m ( $m = 0.674, \omega = 0.304$ )     | Nakagami-m ( $m = 0.821, \omega = 0.213$ )     |
| Right wrist | Walk   | 1     | 90          | Lognormal ( $\mu = -1.13, \sigma = 0.665$ )    | Lognormal ( $\mu = -1.26, \sigma = 0.848$ )    |
| Right wrist | Walk   | 2     | 0           | Lognormal ( $\mu = -0.532, \sigma = 0.228$ )   | Gamma ( $a = 3.36, b = 0.0978$ )               |
| Right wrist | Stand  | 3     | 180         | Normal ( $\mu = 0.93, \sigma = 0.0272$ )       | Lognormal ( $\mu = -0.0516, \sigma = 0.0177$ ) |
| Right wrist | Stand  | 3     | 270         | Lognormal ( $\mu = -0.0953, \sigma = 0.0376$ ) | Normal ( $\mu = 0.96, \sigma = 0.0123$ )       |

Angle orientation of the subject with respect to the receiver, D is horizontal distance from subject to receiver

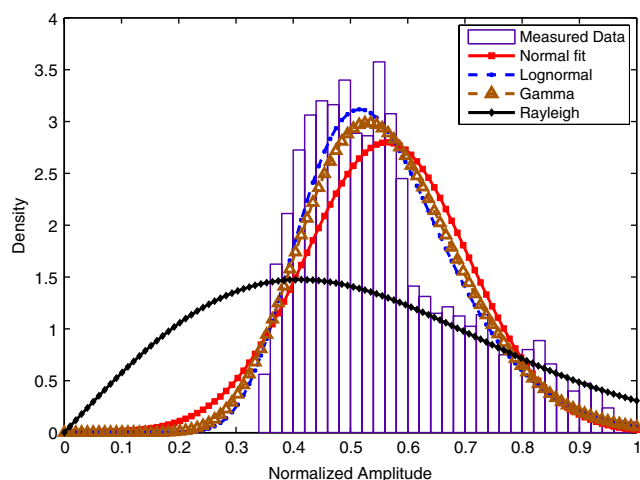


**Fig. 13** PDF back to chest, running, 10 MHz bandwidth at 2.36 GHz

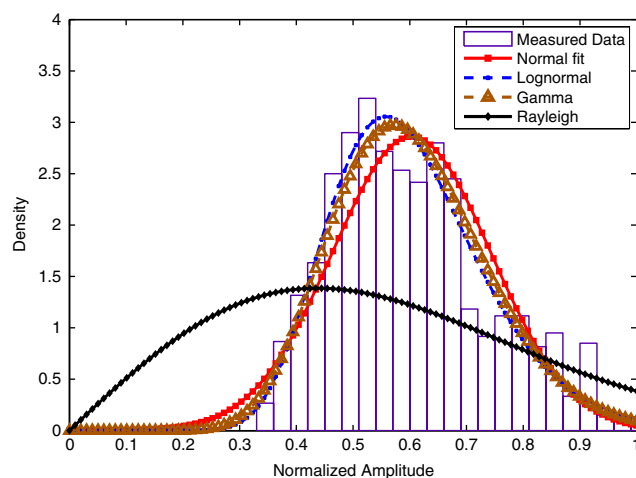


**Fig. 14** PDF right wrist to off-body Rx at 2 m, subject walking, 0° orientation Rx with respect to Tx, 10 MHz bandwidth at 820 MHz

data samples (note: Although parameters may change with distributions fitted with normalization to the maximum amplitude, rather than rms amplitude, the best fitting distribution itself should not change). A sample of best fits for the 10-MHz bandwidth on-body measurements in Table 5,<sup>7</sup> and in Table 6 for off-body measurements.<sup>8</sup> These fits are indicative of the general trend for lognormal models to be the best fitting to individual transceiver link measurements at the 10-MHz bandwidth.

In Fig. 13, an empirical PDF, with best fits overlaid, of normalized (to maximum) received amplitude for an individual on-body link measurement from Tx at back to Rx at chest, with subject running, for 10 MHz bandwidth at 2.36 GHz of measurement case 1. It is evident, as elucidated in the sample results Table 5, that the lognormal distribution is the best fit; this is typical for individual link measurements at this 10-MHz bandwidth. In Fig. 14, an empirical PDF, with best fits overlaid, of normalized (to maximum) received amplitude for an individual off-body link measurement from Tx at right wrist to Rx off-body at 2 m distance, with subject walking, with subject wearing Tx facing Rx for 10 MHz bandwidth, at 820 MHz, of measurement case 2.<sup>9</sup> Once again the lognormal best fit is evident. However, it is also evident that the Gamma best fit is close to the Lognormal best fit in both cases of Figs. 13

and 14, and this is typical and gives a certain strength of evidence for using the Gamma distribution as a generic case for the dynamic scenarios, considering its' reasonable match to individual link measurements.

#### 3.4 Individual link-data first-order statistical analysis—observations

We focus our observations for individual link analysis based on the results for the 10-MHz larger bandwidth, described in the previous subsection. In terms of individual link measurements at the larger bandwidth, the Lognormal distribution is in general the best-fitting statistical model. This is for the same reasons as those shared in [23]. There is a large number of effects contributing to the attenuation of the transmitted signal, such as diffraction, reflection, energy absorption, antenna losses, etc. At this bandwidth, in general, these effects are multiplicative, or equivalently additive in the log domain. By the central limit theorem, a large number of random multiplicative effects will converge to a normal distribution in the log domain. Due to the office environment and also around the body, there are likely to be additive effects due to combination of multiple paths. It is shown in [34] that adding together Lognormal variables results in a distribution that can be well approximated by another Lognormal distribution. Thus, if describing an individual link at a larger bandwidth of 10 MHz (although still narrowband), the Lognormal distribution provides a good approximation.

It is apparent that the dominant model for given link measurement, i.e., Lognormal, particularly at the higher bandwidth, is relatively independent of

<sup>7</sup>The complete set of on-body fits is in [5].

<sup>8</sup>The complete set of off-body fits is in [6].

<sup>9</sup>This case is specified in the seventh row of Table 6, in the column for 820 MHz.

transceiver location.<sup>10</sup> For any given link measurement, best-fitting models are independent of line-of-sight/non-line-of-sight scenarios, which has been elucidated from analysis of all links in [5, 6].

Further, although Lognormal distribution most often provides the best fit out of distributions tried for individual link measurements with a bandwidth of 10 MHz, using the Gamma distribution often provides a reasonable fit, where the corresponding agglomerate scenario best-fitted distribution is a Gamma distribution. Similarly, the Weibull distribution often provides a reasonable fit where the corresponding agglomerate scenario best-fitted distribution is a Weibull distribution. Thus, we postulate it is a reasonable approximation to apply the resulting models for agglomerate scenarios to any individual link measurements at the larger bandwidth.

#### 4 Dynamic narrowband on-body channel: temporal second-order statistics

In order to complement previous first-order statistical analysis, we present two important second-order temporal statistics, *fade duration* and a novel measure, called *fade magnitude*. We present these measures for continuous data at 427, 820, and 2,360 MHz and the channel sounder measurements, for the on-body channel, hence the 100-kHz bandwidth for measurement cases 1 and 3 and 540-kHz bandwidth for case 4. These measures were derived from all the movement data and the general channel sounder measurements.

*Fade duration* is the continuous duration of any interval when the received signal power drops below the mean received signal power, during any given measurement set.

Using the second-order Akaike information criterion as the measure (Eq. 7), we attempted to fit five of the same distributions as applied in first-order statistical analysis, i.e., the Lognormal, Normal, Weibull, Gamma, and Nakagami-m distributions, for each of the continuous agglomerate 100-kHz bandwidth measurements, at each carrier frequency of 427, 820, and 2,360 MHz, and the channel sounder 540-kHz bandwidth at 2,360 MHz. We fit these distributions directly to the fade duration data. A summary of the best-fitting distributions and their relevant parameters is given in Table 7.

Note that the first-order statistics in conjunction with direct fits to fade duration and fade magnitude,

**Table 7** Summary of best fits to continuous, 100 kHz bandwidth, on-body fade duration data at 427, 820, and 2,360 MHz, and the channel sounder 540-kHz bandwidth, fade duration data

| Action     | Frequency (MHz) | Fade duration distribution                 |
|------------|-----------------|--|
| Moving     | 427             | Weibull ( $a = 0.258, b = 0.842$ )         |
| Moving     | 820             | Gamma ( $a = 0.688, b = 0.337$ )           |
| Moving     | 2,360           | Weibull ( $a = 0.0977, b = 0.521$ )        |
| Various-CS | 2,360           | Lognormal ( $\mu = -2.60, \sigma = 1.71$ ) |

along with average level crossing rate define second-order statistics, incorporating all small-scale deviations with respect to all thresholds below the mean, and in conjunction with first-order statistics can be used to regenerate typical small-scale fading power profiles.

The empirical PDF of measured fade durations for the 427-MHz measurements with movement, along with the Weibull distribution best fit to these fade statistics, as described in Table 7, is given in Fig. 15. Accordingly for 427 MHz measurement, the expected fade duration with respect to the mean is 0.28 s. The empirical of measured fade durations for the channel sounder 2,360-MHz measurements, along with the Lognormal distribution best fit to these fade statistics, as described Table 7, is given in Fig. 16. According to this best fit, the expected fade duration is 0.33 s.

*Level crossing rate* is another statistic of some importance, which we define as the average rate at which the signal crosses into a fade (i.e., goes below the mean).

1. Overall measurements at 427 MHz, 100 kHz bandwidth, the average level crossing rate, with respect to the mean signal level over each set of measurements was 2.36 Hz.

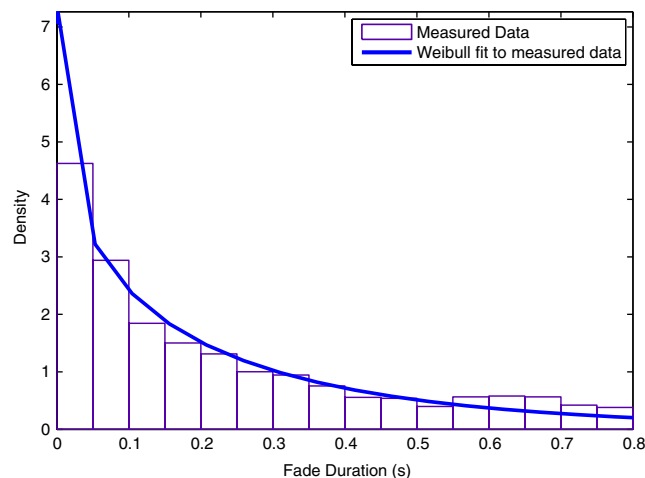


**Fig. 15** Empirical data of measured fade durations, for 427 MHz movement data, with best fit Weibull distribution overlaid

<sup>10</sup>Although there will be some variation in parameters for each link.

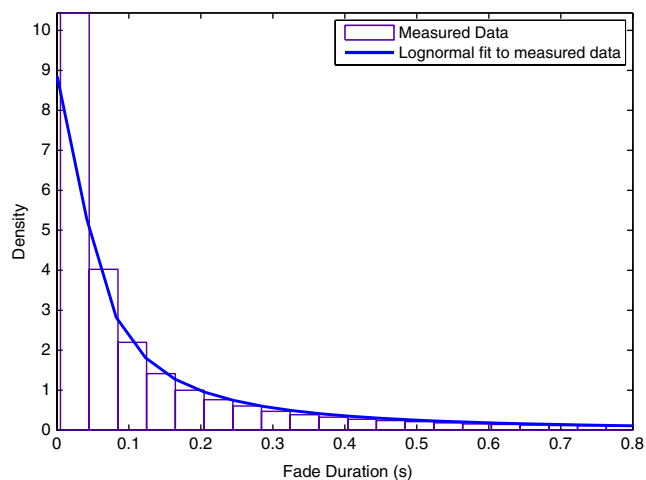


**Fig. 16** Empirical data of measured fade durations, for channel sounder, 2,360 MHz, everyday activity data with best fit Lognormal distribution overlaid

2. At 820 MHz for the treadmill measurements, 100 kHz bandwidth, the level crossing rate is 2.69 Hz.
3. At 2,360 MHz, 100 kHz bandwidth, with movement, this level crossing rate is 3.73 Hz.
4. For the channel sounder at 2.36 GHz, 540 kHz bandwidth, with everyday activity this level crossing rate is 2.2 Hz.

In all cases, this level crossing rate is near to the peak value for all thresholds (i.e., the peak LCR occurs for a threshold level a few decibels below the mean). The LCR at the threshold of the mean (as it is close to the peak LCR) for the fading channels observed here can be used to obtain an estimate for Doppler spread; thus, 3 Hz→4 Hz is a reasonable approximation for average Doppler spread in the body area channel.

We propose one further important second-order statistic that we consider to give further appropriate characterization of the BAN channel dynamics, which we call “fade magnitude”.

*Fade magnitude* is the maximum fade depth with respect to the mean (hence this magnitude is a value greater than 0 dB), during the period of any fade. The fade magnitude is an important indicator of the level of attenuation a signal may encounter when it enters a fade.

In the case of the 100-kHz bandwidth measurements, those not from the channel sounder, the measurement process enabled the capture of very deep fades. In order to facilitate analysis, we again characterize the fade magnitude with an empirical PDF; it was found that there was no common statistical distribution that would fit well to the linear values of fade magnitude,

**Table 8** Summary of best fits to continuous, on-body fade magnitude data at 427, 820, and 2,360 MHz, all 100 kHz bandwidth, and the channel sounder 540-kHz bandwidth, fade magnitude data

| Action     | Frequency (MHz) | Fade magnitude distribution                   |
|------------|-----------------|---|
| Moving     | 427             | Gamma-dB ( $a = 0.713, b = 13.41$ )           |
| Moving     | 820             | Gamma-dB ( $a = 0.669, b = 14.5$ )            |
| Moving     | 2,360           | Gamma-dB ( $a = 0.296, b = 30.1$ )            |
| Various-CS | 2,360           | Lognormal-dB ( $\mu = 0.858, \sigma = 1.13$ ) |

including many other statistical distributions, such as the extreme-value distribution. However, attempting to fit the five common statistical distributions that are often applied to fading channel gain statistics, which were also used to fit to fade durations, it was found that there was a very good fit of some of the five distributions above to the decibel values of fade magnitude, we call these “-dB” fits, once again the Akaike criterion was used to compare between fits. *These distributions are directly fitted to fade magnitude data.* These best fits are given in Table 8; for the three sets of continuous data, those not from the channel sounder, these are “Gamma-dB” fits, and for the channel sounder, this is a “Lognormal-dB” fit.

The empirical PDF of fade magnitude and the Gamma-dB fit for the 820-MHz treadmill measurements are shown in Fig. 17. The empirical PDF of fade magnitude and the Lognormal-dB fit for the channel sounder is shown in Fig. 18.

If generating random appropriate fade magnitudes, random decibel values  $f_{md}$  from a Gamma (or lognormal) distribution with specified  $a$  and  $b$  (or  $\mu$  and  $\sigma$ ) in Table 8 can be generated (by using MATLAB’s

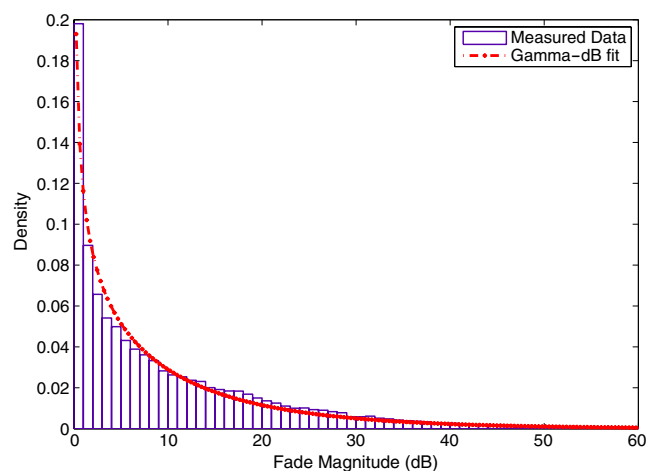


**Fig. 17** Empirical data of measured fade magnitudes for 820-MHz treadmill measurements, with Gamma distribution best fit to the decibel values overlaid

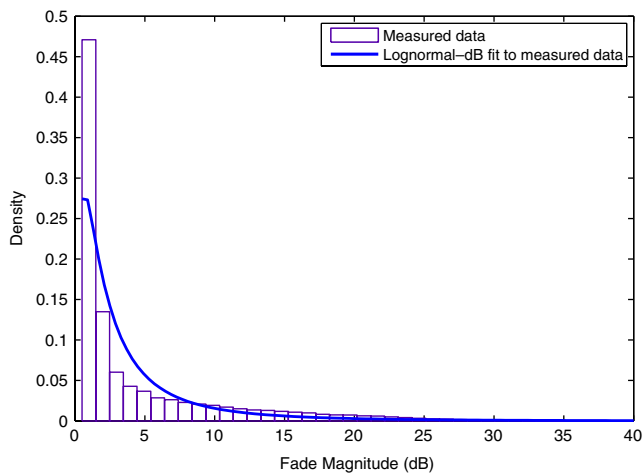


**Fig. 18** Empirical data of measured fade magnitude, for channel sounder, 2,360 MHz, everyday activity data, with Lognormal distribution best fit to the decibel values overlaid

gamrnd, or MATLAB's lognrnd, commands for instance), and if absolute magnitude is required, the conversion  $f_m = 10^{(f_{md}/10)}$  can simply be used.

## 5 Concluding remarks

First- and second-order statistical characterization of the human body area propagation channel has been presented, which has application to inform the design of wireless body sensor networks, with a variety of applications such as biomedical monitoring and sports performance analysis. The set of characterizations is comprehensive, close to two candidate ISM frequencies for BAN, that is, 900 and 2,400 MHz, and close to the implant communications medical implant communications band at 402 MHz.

We make some general claims and observations based on our large number of measurement campaigns

- Median (rather than mean) path loss is a preferable guide for BAN applications [35], which varies according to carrier frequency, and at 2.4 GHz is approximately 70 dB for a generic link
- Movement dominates any small-scale fading model [13] such that the small-scale variations in signal strength are generally movement induced
- For first-order fits of agglomerated data:
  - The given statistical models were “good” fits, with Weibull or Gamma typically best
  - Rayleigh statistical models were a poor fit to measured data

- Best fits were independent of non-line-of-sight and line-of-sight conditions and carrier frequency
- For models of agglomerate data, the best fits were independent of bandwidth (whether 100 kHz, 540 kHz, or 10 MHz)
- For second-order fits of agglomerated data:
  - The given statistical models were “good” fits, especially for fade duration and fade magnitude
  - Fade-duration fitted Gamma or Weibull for periodic activity and log-normal for “everyday” channel sounder measurements
- Based on second- and first-order statistics observed, the body area radio channel is a slow fading channel

Using standard distributions to describe radio channel fading characteristics, it is demonstrated that there is significant structure of the receive signal power profile in the on-body and off-body BAN channel. Thus, in the general case, it can be best modeled by either a Gamma distribution or a Weibull distribution. The Lognormal distribution provides a good fitting model for many individual link measurements for larger bandwidth, but even in these cases the Gamma distribution provides a reasonable approximation. It is demonstrated that best fitting models, where a model represents a distribution type, to agglomerate data, are not indicated by bandwidth (when narrowband), or by scenario, such as on-body walking or off-body walking, or by carrier frequency; nor are their parameters indicated by bandwidth or carrier frequency.

Second-order temporal statistics of fade duration and fade magnitude (or fade depth) have also been modeled at the three potential BAN carrier frequencies; it is demonstrated that these statistics can be well modeled by the same distributions (of course with different parameters for those distributions) as those applied to first-order statistics; the distributions are Lognormal, Gamma, and Weibull.

It is considered that the analysis presented here is readily applicable to many typical narrowband BAN radio systems design and evaluation, and in that respect, there is significant potential future application of the analysis that has been presented here. The channel sounder data and hence its' characterization incorporate some outdoor body area measurement data, but there is further potential work in obtaining more outdoor measurements; and doing specific analysis of the on-body and the off-body area channel in an outdoor environment.

## Appendix

Variance of the Gamma distribution, shape parameter  $a$ , scale parameter  $b$

$$\text{Var}_{\text{gam}}(x) = ab^2. \quad (8)$$

Variance of the Weibull distribution, scale parameter  $a$ , shape parameter  $b$

$$\text{Var}_{\text{wbl}}(x) = a^2 \left[ \Gamma \left( 1 + \frac{2}{b} \right) - \Gamma^2 \left( 1 + \frac{1}{b} \right) \right]. \quad (9)$$

Variance of the Nakagami- $m$  distribution, shape parameter  $m$ , spread parameter  $\omega$

$$\text{Var}_{\text{nak}}(x) = \omega \left( 1 - \frac{1}{m} \left( \frac{\Gamma(m + 1/2)}{\Gamma(m)} \right)^2 \right). \quad (10)$$

## References

- Miniutti D, Hanlen L, Smith D, Zhang A, Lewis D, Rodda D, Gilbert B (2008) Dynamic narrowband channel measurements around 2.4 GHz for body area networks. IEEE802.15.6 technical contribution, document ID: 15-08-0354-01-0006-dynamic-narrowband-channel-measurements-around-2-4-ghz-for-body-area-networks
- Miniutti D, Hanlen L, Smith D, Zhang A, Lewis D, Rodda D, Gilbert B (2008) Narrowband on-body to off-body channel characterization for body area networks. IEEE802.15.6 technical contribution, document ID: 15-08-0559-00-0006-narrowband-On-Body-to-Off-Body-channel-characterization-for-ban.pdf
- Miniutti D, Hanlen L, Smith D, Zhang A, Lewis D, Rodda D, Gilbert B (2008) Characterisation of small-scale fading in BAN channels. IEEE802.15.6 technical contribution, document ID: 15-08-716-00-0006
- Miniutti D, Hanlen L, Smith D, Zhang A, Lewis D, Rodda D, Gilbert B (2009) NICTA proposal. IEEE802.15.6 technical contribution, document ID: 15-09-0345-00-0006
- Smith D, Hanlen L, Miniutti D, Zhang J, Rodda D, Gilbert B (2008) Statistical characterization of the dynamic narrowband body area channel. In: Applied sciences on biomedical and communication technologies. First international symposium on ISABEL '08, pp 1–5. doi:10.1109/ISABEL.2008.4712618
- Smith D, Hanlen L, Zhang J, Miniutti D, Rodda D, Gilbert B (2009) Characterization of the dynamic narrowband on-body to off-body area channel. In: IEEE international conference on communications. ICC '09, pp 1–6. doi:10.1109/ICC.2009.5198824
- Smith D, Miniutti D, Hanlen L, Zhang JA, Rodda D, Gilbert B (2009) Dynamic channel measurements around 400 MHz for body area networks. IEEE802.15.6 technical contribution, document ID: 15-09-0186-00-0006-dynamic-channel-measurements-around-400mhz-for-body-area-networks.pdf
- Zhen B, Patel M, Lee S, Won E (2008) Body area network (BAN) technical requirements. 15-08-0037-01-0006-ieee-802-15-6-technical-requirements-document-v-4-0
- Lewis D (2008) IEEE P802.15-08-0407-05: 802.15.6 call for applications—response summary. IEEE submission
- Hall PS, Hao Y (2006) Antennas and propagation for body centric wireless networks. Artech, Norwood
- Yazdandoost KY, Sayrafian-Pour K (2008) Channel model for body area network (BAN) [IEEE-802.15-08-0033-00-0006]. NICT, NIST
- Scanlon WG, Evans NE (2001) Numerical analysis of body-worn UHF antenna systems. IEEE Electron Commun Eng J 13:53–64
- Miniutti D, Hanlen LW, Smith DB, Zhang JA, Lewis D, Rodda D, Gilbert B (2008) Narrowband channel characterization for body area networks [ieee-208.15.08.0421.00.0006]. Tech. rep., IEEE802.15.6
- Gupta SKS, Lalwani S, Prakash Y, Elsharawy E, Schwiebert L (2003) Towards a propagation model for wireless biomedical applications. In: IEEE global communications conference. GLOBECOM 2003, pp 1993–1997
- Smith DB (2008) Electromagnetic characterisation through and around human body by simulation using SEMCAD X. Tech. rep. CRL-3282, NICTA
- Fort A, Desset C, Wambacq P, Biesen L (2007) Indoor body-area channel model for narrowband communications. IET Microwaves Antennas Propag 1(6):1197–1203
- Zasowski T, Meyer G, Althaus F, Wittneben A (2005) Propagation effects in UWB body area networks. In: 2005 IEEE international conference on ultra-wideband, 2005. ICU 2005, pp 16–21
- Obayashi S, Zander J (1998) A body-shadowing model for indoor radio communication environments. IEEE Trans Antennas Propag 46(6):920–927. doi:10.1109/8.686781
- Hall P, Hao Y, Nechayev Y, Alomalny A, Constantinou C, Parini C, Kamarudin M, Salim T, Hee D, Dubrovka R, Owadally A, Song W, Serra A, Nepa P, Gallo M, Bozzetti M (2007) Antennas and propagation for on-body communication systems. IEEE Antennas Propag Mag 49(3):41–58. doi:10.1109/MAP.2007.4293935
- Neiryck D, Williams C, Nix A, Beach M (2004) Wide-band channel characterisation for body and personal area networks. In: 2nd international workshop on wearable and implantable body sensor networks
- Cotton SL, Scanlon WG (2006) A statistical model for indoor multipath propagation for a narrowband wireless body area network. In: IEEE personal, indoor and mobile radio communications symposium, PIMRC 2009, pp 1–5
- Cotton SL, Scanlon WG, Jim G (2008) The  $\kappa - \mu$  distribution applied to the analysis of fading in body to body communication channels for fire and rescue personnel. IEEE Antennas Wirel Propag Lett 7:66–69
- Fort A, Desset C, de Doncker P, Wambacq P, van Biesen L (2006) An ultra-wideband body area propagation channel model-from statistics to implementation. IEEE Trans Microwave Theory Tech 54(4):1820–1826
- Scanlon WG, Cotton SL (2008) Understand on-body fading channel at 2.45 GHz using measurements based on user state and environment. In: Loughborough antennas and propagation conference, pp 10–13. Loughborough, UK
- Zhang QT (2003) A generic correlated Nakagami fading model for wireless communications. IEEE Trans Commun 51(11):1745–1748
- Ganesh R, Pahlavan K (1989) On the modeling of fading multipath indoor radio channels. In: IEEE global communications conference. GLOBECOM 1989, vol 3, pp 1346–1350

27. Akaike H (1973) Information theory as an extension of the maximum likelihood principle. In: Proc. 2nd. int. inf. theory syst., pp 267–281
28. Burnham K, Anderson D (2002) Model selection and multi-model inference: a practical information-theoretic approach, 2nd edn. Springer, Berlin (2002)
29. Freedman D, Diaconis P (1981) On the histogram as a density estimator:  $L_2$  theory. Probabi Theory Related Fields 57(4):453–476
30. Hashemi H (1993) The indoor radio propagation channel. Proc IEEE 8(7):943–968. doi:[10.1109/5.231342](https://doi.org/10.1109/5.231342)
31. Tzeremes G, Christodoulou C (2002) Use of Weibull distribution for describing outdoor multipath fading. In: Antennas and Propagation Society international symposium, vol 1. IEEE, New York, pp 232–235. doi:[10.1109/APS.2002.1016291](https://doi.org/10.1109/APS.2002.1016291)
32. Abdi A, Kaveh M (1999) On the utility of gamma pdf in modeling shadow fading (slow fading). In: IEEE 49th vehicular technology conference, vol 3, pp 2308–2312. doi:[10.1109/VETEC.1999.778479](https://doi.org/10.1109/VETEC.1999.778479)
33. Abdi A, Kaveh M (1999) Envelope PDF in multipath fading channels with random number of paths and nonuniform phase distributions. In: Tranter WH, Rappaport TS, Wornner BD, Reed JH (eds) Wireless personal communications. Kluwer, Norwell, pp 275–282
34. Fenton L (1960) The sum of log-normal probability distributions in scatter transmission systems. IEEE Trans Commun Syst CS-8(1):57–67
35. Hanlen LW, Miniutti D, Rodda D, Gilbert B (2009) Interference in body area networks: distance does not dominate. In: IEEE personal indoor and mobile radio conference. PIMRC 2009. Yokohama, Japan